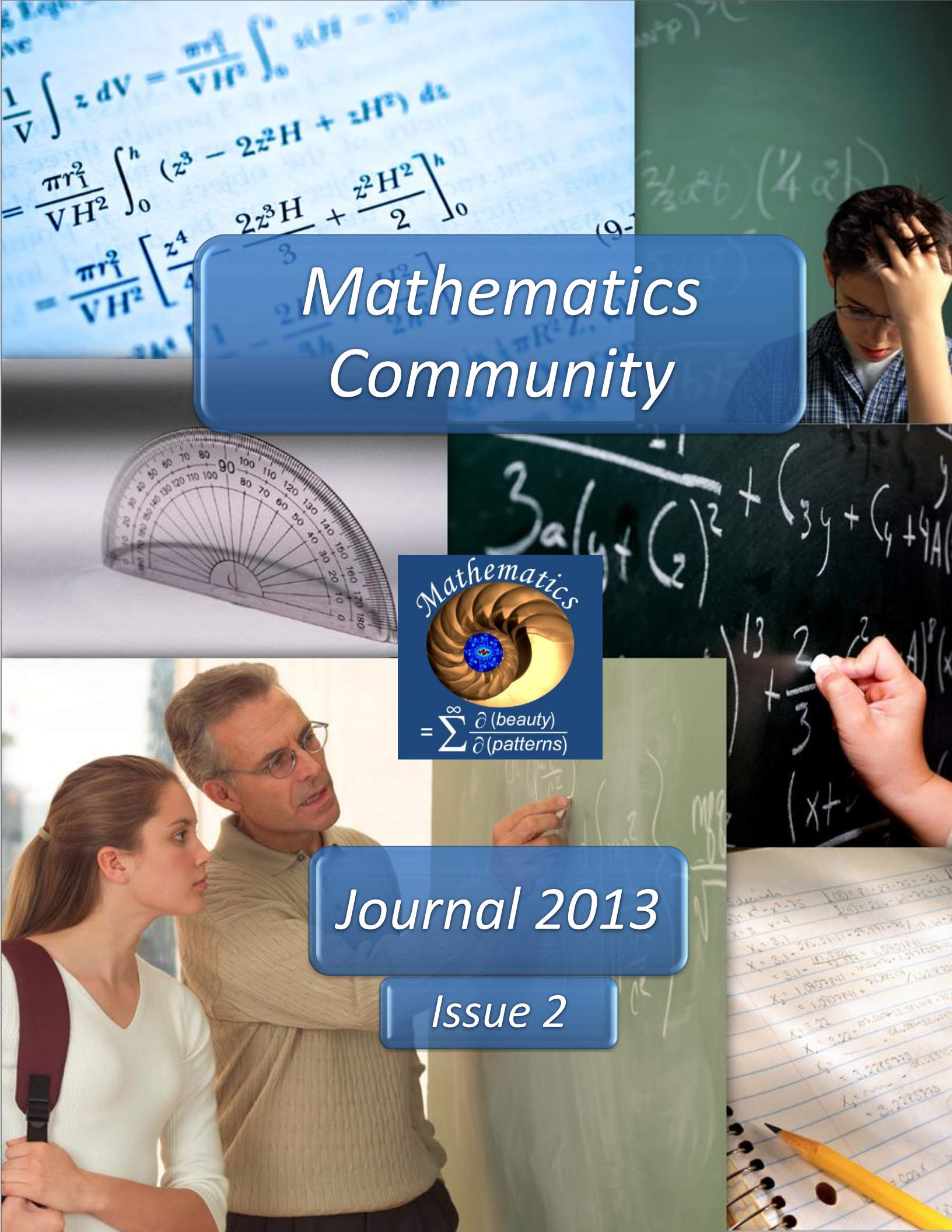

Mathematics Community

Journal 2013

Issue 2

From The Community Leaders

Dear Schlumberger Mathematics Community Members! First of all, we would like to thank all the members who participated in different Mathematics Community activities. A special thanks to all that wrote articles for this Journal. We also would like to congratulate everyone with the **15-year Eureka anniversary!**

We are pleased to present the new issue Mathematics Community Journal. This journal consists of mathematics related articles that have been written by Schlumberger employees. If you would like to provide your feedback to authors, find them in corporate address book. All the community members and other Schlumberger mathematicians are welcomed to submit papers for next Journal issues!

About the Community. Currently, the Mathematics Community has 6 SIGs: Applied Mathematics SIG, Geometric Modelling SIG, Inversion Optimization and Uncertainty SIG, Mechanical CAD SIG, Modelling and Imaging SIG and Ocean SIG. We have **1430 members**. There are **4 Fellows**, **28 Advisors**, **74 Principals** and **285 Seniors** in the Community. From the total number of members joined the Community, there are 33 Community/SIG leaders: **1 Advisor**, **4 Principals**, **23 Seniors** and **5 Eureka members**. The distribution of members by segment by country presented below:

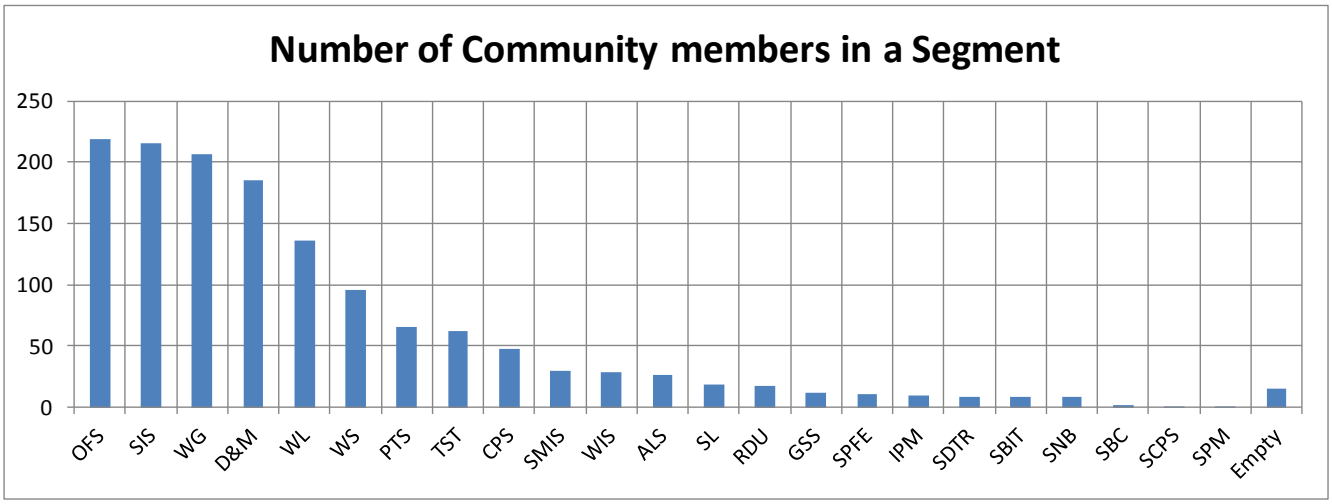

Figure 0.a - The distribution of Community members by segment

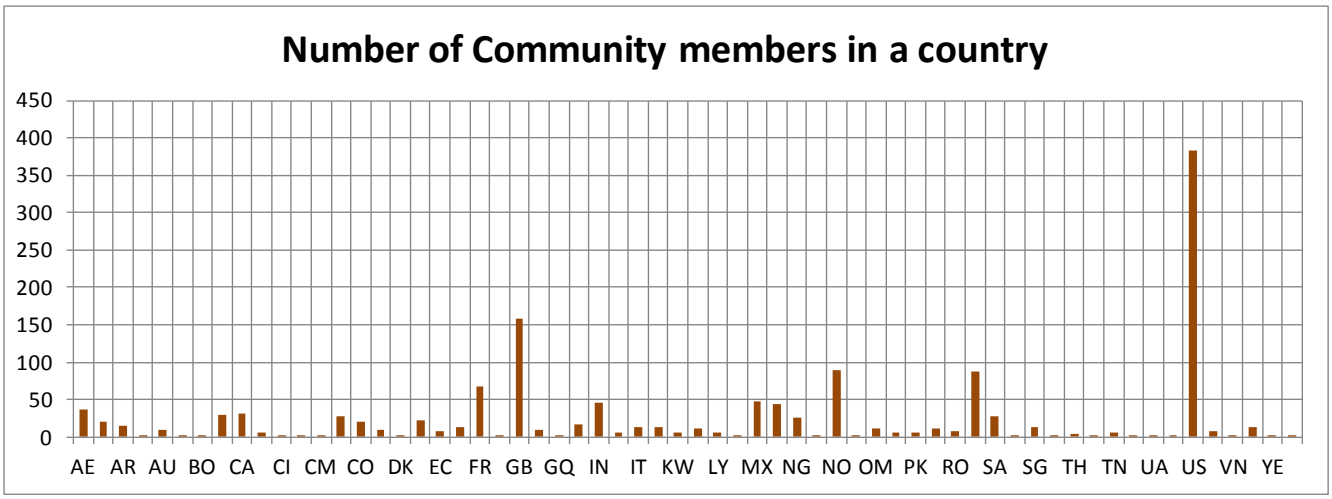

Figure 0.b - The distribution of Community members by country

This Journal consists of the following articles:

We really encourage you to submit articles to SIGs and Community Newsletters, technical reviews, interesting news, etc., as we think it is an excellent way of sharing knowledge and giving visibility to projects and people.

Best regards,

Børre & Alexander

Mathematics Community Leaders 2013

Authors

Alejandro Cortés Cortés, Well Engineer, IPM Well Constructions, Rio de Janeiro, Brasil

Alexander Kuvichko, Reservoir Engineer, PTS, Megion, Russia;
Mathematics Community Leader, 2013

Ascencio Cendejas, National Autonomous University of Mexico-Petroleos Mexicanos

Børre Bjerkholt, Project Architect for Petrel Drilling Integration Task Force, Project Architect for Geology & Modeling Team, SIS, Norway;
Mathematics Community Leader, 2013

Halvor Sehested Groenaas, WOTC, Oslo, Norway

Igor Magdeev, Senior Reservoir Engineer, PTS Mos-cow, Russia

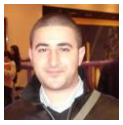

Reda Badache, Information Management Technical Team Leader, SIS, Cheraga, Algeria

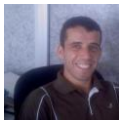

Redha Benyamina, SIS-IM Engineer, SIS, Hassi Messaoud, Algeria

Tahar Amine Mostefaoui, RIG Support Team Leader, SIS, Hassi Messaoud, Algeria

Terry Miller, Marketing Communications, Houston-Richmond, US

Table of Contents

Grain Size Analysis: Revitalizing the Technique for Micro-scale Reservoir Rock Characterization

Igor Magdeev, Senior Reservoir Engineer,
PTS Moscow, Russia

Abstract

The title problem is one of the keys in the understanding of the reservoir rock structure and properties. For the unconsolidated sandstone the issue is formation rock failure under changing stress state due variation of pressure drawdown. The possible consequent sand production requires solutions for completion design procedure and for the particular rheological problems of the solid suspension flow. Several technical articles' authors developed the complex solid transport models, but rarely the core data measurements are mentioned [1, 2 and 3]. For both disciplines the very important grain size analysis data is typically reduced to the single number only – median of grain size distribution.

This looks like a 'bottleneck' connection between different domains. Meanwhile, the core samples are much richer of information that can be extracted for various modeling purposes: from reservoir characterization on the micro-scale to the production technology issues like erosion and solid transport. Although, the number of observations on the core samples usually limited, the careful data processing being done enables significant increase of the information value.

This study is dedicated to the application of finite mixture modeling tools – one of the popular approaches in data mining with particular orientation to the core data.

Problem statement and solution workflow

Modern reservoir characterization case studies often performed using probabilistic tools [4]. The objective of this work is to establish the workflow for processing of core data with sufficient output for reservoir modeling purposes.

Although, in the engineering handbook one can find examples presenting simple picture of reservoir rock particle size [5], typically for general case, the grain size distribution can be expressed as complex multi-modal mixture of individual components. The numerical simulations of such grain size samples may be performed using well known finite mixture modeling techniques. To be able to implement such simulation one should have the estimation of parameters: the number of components in mixture n; the parameters of each individual distribution and the proportions of each component in overall mixture.

The solution workflow is described below and consists of the following steps:

1) Prepare core analysis data
2) Estimation procedure of mixture model parameters
3) Result validation and analysis
4) Post-processing, overview and discussion
5) Conclusions and propositions for future

1. Prepare core analysis data

The grain size analyses may be performed using various techniques: dry or wet sieve tools, laser diffraction, settling columns, either bulk sampling [6]. Typically, distributions from core samples measured using laser diffraction method have better resolution.

The laser light scattering technique involves an inverse problem solution with important assumptions: normality of the solid particle size distribution in log scale and sphericity of particles themselves.

But, in the output client report one can usually obtain only the final summary data viz. on Figure 1. The problem in a nutshell is "to teach the machine what engineer can see".

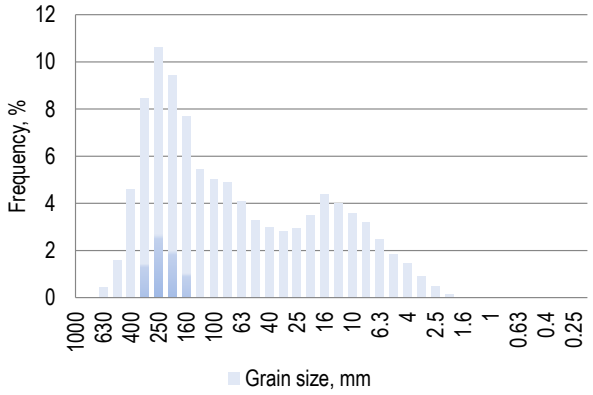

Figure 1 – Grain size distribution example: unconsolidated sandstone

Initial data set of the studied field contains 71 core sample grain size measurements with output univariate histograms with 1.25 bin size ratio from 1000 μm down to 0.16 μm. The bin values further will be taken as check-points for model QC.

After log transform of initial data the very important things can be noted:

- the sense of "median grain size" is lost due to multi-modal nature of distribution - particular sandstone consists of several different Grain Types (GT);

- probability density function (PDF) can be expressed as mixture of several normal distributions (as it has been recognized during measurements);
- for the reasonable model complexity the number of components in fitting and simulations was limited to 5.

Once the initial grain size distribution parameters are known from the core data, they can be simulated numerically, which successfully captures the case of multimodal distribution.

2. Estimation procedure of mixture model parameters

The PDF for presented above case of grain size data can be described in terms of normal distribution mixture – the same to assumption used by laser diffraction method:

$$p(x) = \sum_{i=1}^{n} \omega_i N(x, \mu_i, \sigma_i) \qquad (1)$$

with unknown n, ω_i, μ_i and σ_i parameters. This class of problems typically can be solved by Expectation-Maximization (EM) algorithm and its modifications applied to random sample of observed data.

To set up the problem for this particular case it is necessary to create a random sample from the input data (there are no direct raw observations). The following assumption was made for sampling: uniform distribution within each input bin.

To identify mixture parameters for the generated sample there were two algorithms applied:

- Model-based clustering (further named MCLUST) [6];
- Normal mixture EM (further named NMEM) [7].

To derive the optimal number of components from observed sample first algorithm uses Bayesian Information Criterion (BIC) with a penalty based on the number of components and observations:

$$BIC = 2L - n\log m \qquad (2)$$

where L – maximum of the log likelihood function.

The second algorithm can operate in two modes: with random guess and specified initial guess about mixture parameters. Particular workflow implemented three options:

- MCLUST algorithm only;
- NMEM without prior ("unsupervised", random guess);
- NMEM with prior ("supervised", specified initial guess).

The last option is the attempt to improve inverse problem solution by the combination of two methods: specified initial guess for NMEM is taken from output of MCLUST.

3. Result validation and analysis

Typically, the amount of laser diffraction measurements is very limited; thus, it is easy to control all processed samples manually. For the core sample presented above (Figure 1) the inverse solution by 3 methods is viz. on Figure 2.

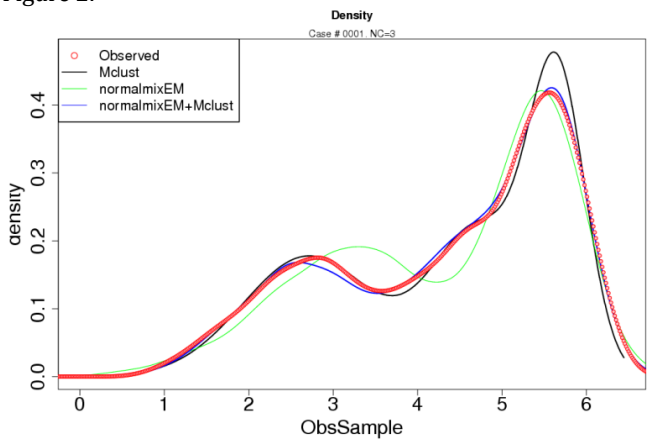

Figure 2 – Visual QC of three fitted models

The key summary points are:

- MCLUST identified 3 components (black line on Figure 2), which corresponds to the maximum BIC value (Figure 3);
- "Unsupervised" NMEM identified only 2 components (green line on Figure 2);
- Finally 3 Gaussian components were identified by "supervised" NMEM with initial guess (blue line on Figure 2).

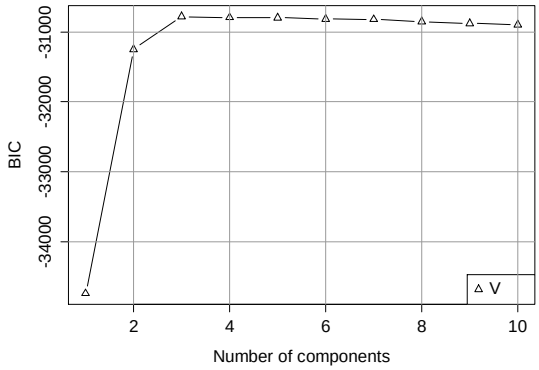

Figure 3 – BIC diagnostic plot

Obviously, from 3 to 6 components BIC values is almost constant, so the preferred model is that one with less complexity. But, "unsupervised" NMEM has poorer result – 2 components is not enough to capture that grain size variation, but output from MCLUST as initial guess for NMEM improves identification of individual parameters, which can also be confirmed by cross-plot with determination $R^2 \geq 0.95$ (Figure 4).

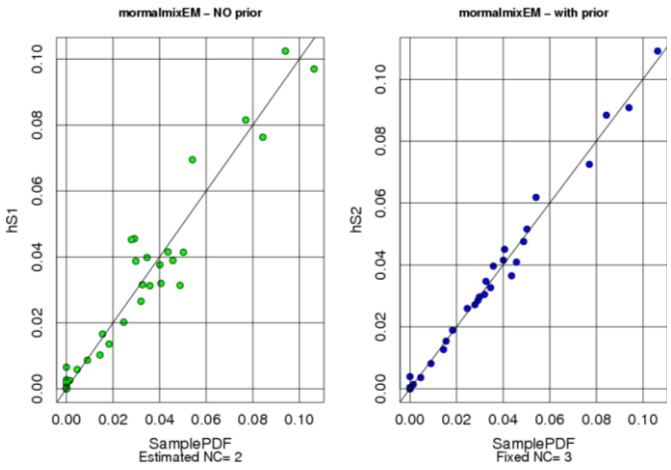

Figure 4 – cross-plot of PDF (normalized to 1) fractions at check-points

The summary of mixture parameters estimation is given below. It can be seen, that mixture parameters variation is small, and two options have their own pros and cons: MCLUST provided very good fit for fine grains fraction, but overestimated peak of the coarse grains, meanwhile NMEM improves estimation of coarse fraction parameters, with less quality of simulation of fine grains.

Table 1 – Summary of mixture parameters

MCLUST				NMEM+MCLUST			
ω_i	μ_i	σ_i^2	d_i^{50}, μm	ω_i	μ_i	σ_i^2	d_i^{50}, μm
0.345	2.7	0.60	15.0	0.338	2.7	0.76	14.6
0.307	4.7	0.32	113.7	0.295	4.7	0.56	107.0
0.348	5.7	0.11	287.3	0.367	5.6	0.34	282.7

Both algorithms performed with a high confidence level of fit to the observed data. There are 3 grain types with distinct median diameter d_{50} values, derived with high similarity (the naming of types is provided in section **4**).

NB: one needs to keep track on the input quality data: the observed sample was not measured, but has been generated based on the histogram, which may contain noise or errors.

Thus, after processing of 71 input core measurements there were obtained two intermediate matrices of mixture parameters for both options: MCLUST and NMEM+MCLUST.

4. *Post-processing, interpretation and discussion*

The grain size classification study using Gaussian multi-component mixture is well described with application to glacial transport of sediments with further attempts to classify sedimentation processes and conditions [6]. For this particular study the interpretation of sedimentation processes goes beyond the objective. However, the result obtained on this stage can form the solid basis for depositional analysis and sedimentary log construction together with core-to-depth data binding.

Once the mixture parameters were estimated for each core sample, the plot of MCLUST output in (μ–σ) coordinates provides a very clear picture (μ – is the measure of grain size and σ – is the measure of sorting [6, 9]). There are 6 disjoint GT obtained by hierarchical clustering method (Figure 5). For the comparison the result from other popular K-means method is provided, and the clusters better recognized by hierarchical method – gray and pink cluster (left picture) were collapsed into one pink (right picture), while the blue cluster of most coarse grains (left) was split into two (right). Also, some "noise" data present between red and green clusters, they may represent a different grain sub-population (!), which was not recognized due to unrepresentative sample data in this area.

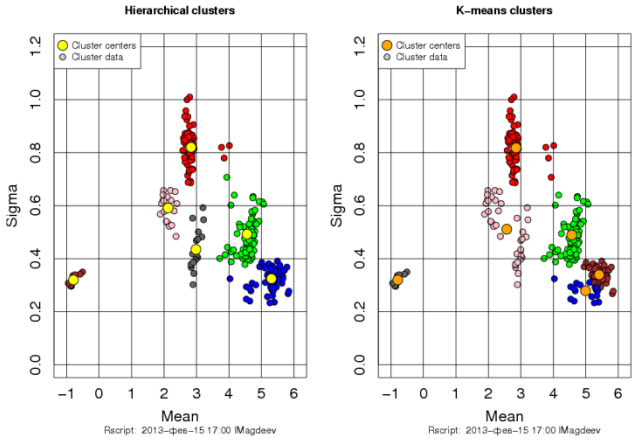

Figure 5 – Grain types clustering after MCLUST processing

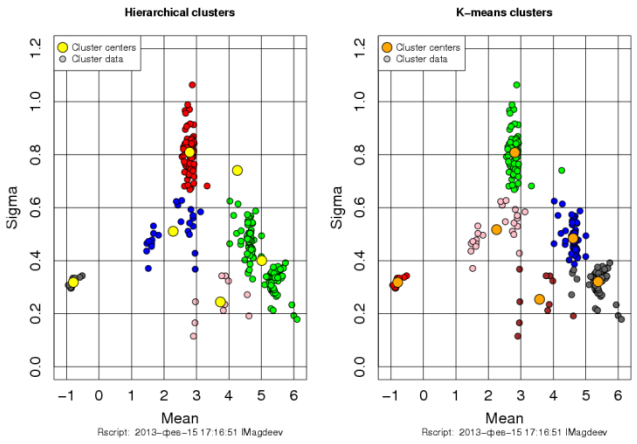

Figure 6 – Grain type clustering after NMEM processing

The NMEM algorithm (on the previous stage) exposed better performance, and the output is also plotted in the same way. The picture became blurred due to much more "noise" occurred in the processed data (Figure 6). This is an indication of the model overlearning or "over fitting"

syndrome. Meanwhile, the K-means method better handled this data, but the number of clusters variation did not improve the final classification.

Consequently, the MCLUST algorithm provides more clear and interpretable result, and can be applied for grain size analyses and studies.

Summary of the grain type classification according to the conventional sedimentology scale is presented below (Table 2). To finalize the classification the description and grade columns were added according to verbal descriptions of the grain size distribution parameters [6, 9]. For all core samples of the studied filed grain sorting is moderate to poor, and may vary within each cluster. The result is also plotted in the conventional scale on the (Figure 7).

Table 2 - Summary of grain size characteristics

Grain type	Size characteristics				Sorting		
	Mean	d_{50} (x_{gi})	Scale	Wentworth Grade	Sigma	σ_{gi}	Description
Units (scale)	log	μm	$\log_2$		log	μm	
I	-0.8	0.5	11	Clay	0.32	1.4	Moderate
II	2.1	8.4	7	Fine silt	0.59	1.8	Moderate
III	2.8	17.0	6	Medium silt	0.82	2.3	Poor
IV	3.0	19.7	6	Medium silt	0.44	1.5	Moderate
V	4.6	95.2	3	Fine sand	0.49	1.6	Moderate
VI	5.3	202.1	2	Medium sand	0.32	1.4	Moderate

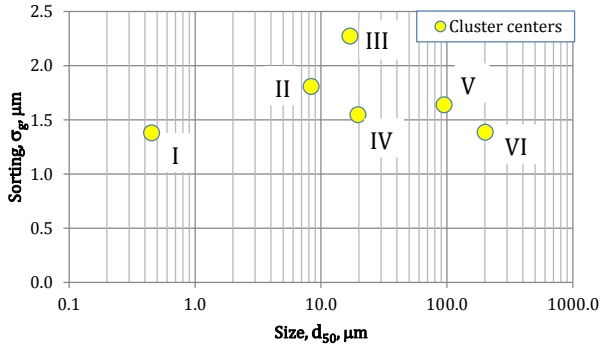

Figure 7 – Final grain types derived from core analysis data

5. Conclusions and propositions for future

The Gaussian mixture approach to the grain size analysis data is well known in the sedimentology [6]. Although it was not frequently used for hydrocarbon reservoir case studies, just limiting the analysis with output for other domain disciplines of single parameter – median grain size.

The laser diffraction method is sufficient for grain size analysis and produces high quality raw data. Even though, the initial data is not presented in report, the grain size distribution parameters can be recovered by solution of the inverse problem of finite mixture modeling.

The established classification of grain types for unconsolidated shallow sandstone formation exposed the importance of comprehensive study due to complex nature of clastic sediments texture.

During the study two modern mathematical algorithms were tested on the available data – model based hierarchical clustering with BIC criterion and standard EM algorithm with maximization of log likelihood function. The model based clustering (MCLUST) produced more robust classification with distinct clearly visible clusters.

Conventional verbal description can assist the understanding of the reservoir sediments, but is not sufficient for simulation-oriented problems.

The classification result and finite mixture modeling parameters can be proposed for further application in the following geo-engineering subject matter:

- Thin sections analyses and enhanced micro-scale rock characterization;
- Petrophysical rock typing and porosity-permeability relationship establishing;
- Sand production problems and completion design;
- Flow assurance problems of sand accumulation in horizontal well completion and erosion process modeling.

Nomenclature

The unit system used through this work is metric.

n – number of components in mixture

x_i – random variable denoting i^{th} component in mixture

$N(x, \mu, \sigma)$ – normal distribution PDF of variable x, mean μ and st.dev. σ

ω_i – weight (or proportion) of i^{th} component in mixture

μ_i – location parameter of lognormal distribution of i^{th} component

σ_i – scale parameter of lognormal distribution of i^{th} component

m – number of observations

d_{50} – median grain size

x_{gi} – in "geometric method of moments" [9] size parameter

$$x_{gi} = e^{\mu_i}$$

σ_{gi} – in "geometric method of moments" [9] sorting parameter

$$\sigma_{gi} = e^{\sigma_i}$$

Acknowledgements

This methodology and model has been developed during the field development strategy project execution by PTS segment for the major heavy oil-and-gas asset of the Russian oil company.

Special thanks to developers of the powerful software package for various data mining capabilities and tools – http://r-project.org

References

1. Bello K. O., Oyeneyin M. B. and Oluyemi G. F., “Minimum Transport Velocity Models”, SPE 147045, 2011.
2. Liangwen Zhang and Dusseault M. B., “Sand Production Simulation in Heavy Oil Reservoirs”, SPE 64747, 2000.
3. Van den Hoek P. J. and Geilikman M. B., “Prediction of Sand Production Rate in Oil and Gas Reservoirs: Field Validation and Practical Use”, SPE 95715, 2005.
4. McLellan P. J. and Hawkes C. D., “Application of Probabilistic Techniques for Assessing Sand Production Instability Risks”, SPE 47334, 1998.
5. Renpu and Wan, “Advanced Well Completion Engineering (3rd Edition)”, pp. 22; Elsevier, 2011.
6. Evans D. and Benn D., "Practical Guide to the Study of Glacial Sediments", Routledge, Ch. 3, pp. 55-56, 66-67, 72; 2004, ISBN: 9780340759592.
7. Fraley C. and Raftery A. E., “Bayesian regularization for normal mixture estimation and model-based clustering”. J. Classif., 24(2), pp.155-181; 2007.
8. Benaglia T., Chauveau D., Hunter D. R. and Young D., “mixtools: An R Package for Analyzing Finite Mixture Models." Journal of Statistical Software, 32(6), pp. 1-29; 2009, URL: http://www.jstatsoft.org/v32/i06/.
9. Blott S. J. and Pye K., “Gradistat: a grain size distribution and statistics package for the analysis of unconsolidated sediments”, Earth Surf. Process. Landforms 26, pp.1237–1248; 2001, DOI: 10.1002/esp.261.

Planning Optimization Process

Tahar Amine Mostefaoui, RIG Support Team Leader, SIS, Hassi Messaoud, Algeria

Redha Benyamina, SIS-IM Engineer, SIS, Hassi Messaoud, Algeria

Reda Badache, Information Management Technical Team Leader, SIS, Cheraga, Algeria

Introduction

This document describes in details the work that has been done in modeling and resolving mathematically the scheduling jobs versus resources availability problematic.

In fact the RTOM project is one on the most challenging project in terms of managing humans and materials resources as it's the world wide biggest project in terms of rig monitored at the same time (up to 42 rigs), the project that has been implemented based on mathematics knowledge in order to respond to clients need which is connecting rigs and services companies to the remote operations center and streams real time data in proper and perfect data quality.

The main Rig support Team mission is bringing all streamed data from the rig site to the remote operations center, controlling its quality and maintaining the streaming infrastructure.

The Rig Support Team count 8 rig support specialist (Contractors) and 1 Team Leader (Schlumberger Employee), as the most of the team member doesn't have Schlumberger culture that consist in excellence in execution at all job delivery aspect, a lean methodology has been adopted to face the issues related to the objective.

The main pillars of the rig support entity are planning and operations logistic and job delivery quality, where we need to maintain a high level of service delivery quality.

Problematic

The operational objectives for the rig support team is to connect the WSDH boxes within 5 days after the well SPUD and stream 95% of the auxiliary drilling operations (Non Drilling Jobs) such as logging, cementing, MWD, LWD…

In 2011 the project dispose of 4 rig support specialist at any time during the year, the client demand at that time was 15.5 Job/month, the below section give you a picture about the rig support team and the logistics management system performance:

2011 statistics:

- 46% cancelled non drilling job
- 25% cancelled non drilling jobs due to lake of resources
- 2.5 sigma of quality level (Quality = Response to Jobs demand)
- Logistic process takes 3+h/day
- No logistic cost tracking
- Client complaint letter

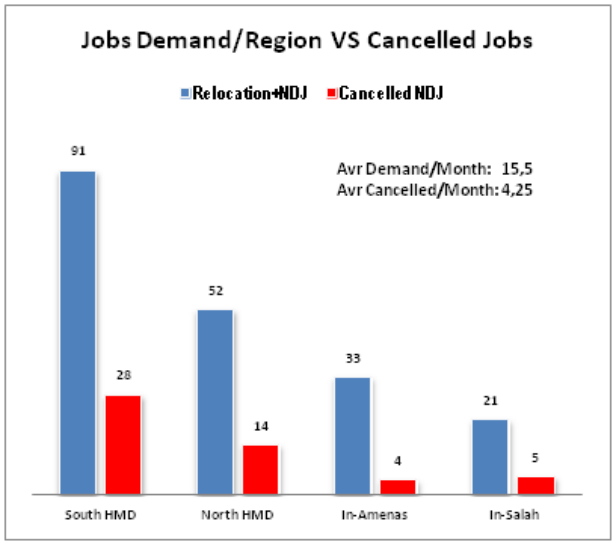

Figure 8 – Jobs Demand/Region VS Cancelled Jobs.

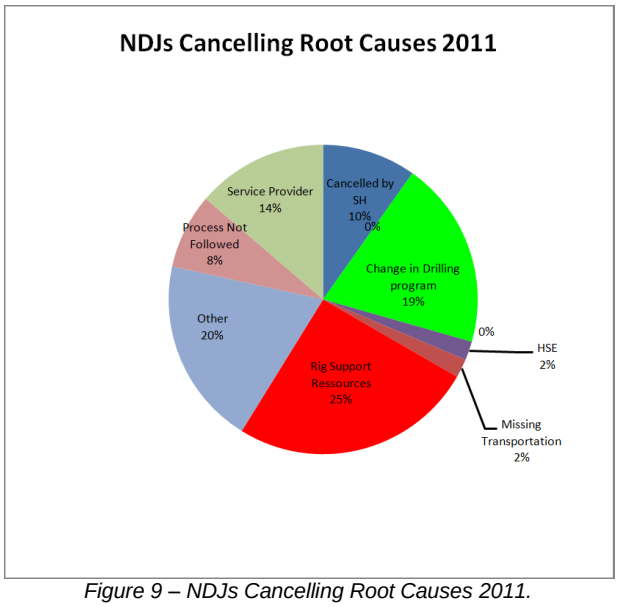

Figure 9 – NDJs Cancelling Root Causes 2011.

Based on this statistic the common sense would say that we were in lack of resources, and by filling this gap the problem will be resolved, but what is amazing, is the fact that with 4 rig support specialist we should respond to a demand of 20 Jobs/Month.

Modeling Approach

In order to give a mathematical resolution of the problem described in the previous paragraph, we've used the graph theory to model the situation, as we are dealing with traveling network the graph theory is one of the most powerful tool that can handle this king of problematic, after the modeling phase we can use a bench of algorithm to get our objective from the model such as the well known the shortest way algorithm or the mail man algorithm (i.e.: look for the shortest chain for node **a** to node **b**, or Hamiltonian cycle within the graph (using mathematical terms)).

Before describing the model let pass first by understanding of why we focus the study on the Planning process rather than on providing resources.

Figure 10 – Resources and planning.

Root cause analysis

Before describing the model let pass first by understanding of why we focus the study on the Planning process rather than on providing resources, by analyzing the root causes on the 2011 process performance we distinguished one main issue that lead to the other root causes, and then using the Pareto principal (80/20) we get the focus point to improve the logistic process.

From this analysis, we can easily deduce the mother root-cause that affect our Team performance in term of responding to client requests, in fact in 2011 we were using the FIFO methodology as logistic system which leads to NDJs cancellations and relocations delay.

Mathematical approach

To resolve the FIFO methodology issue we used the graph theory approach, in fact we model the problem in graph and then we define a heuristic that solves the job rotation problematic.

The graph will be the exact copy of the road network use by the team to move between the different rigs that belong to the RTOM project, the map below show the Algeria desert road network (Figure 14).

The graph is defined as follow:

$G = \{N, E, X\}$,

$N = \{Hassi\ Messaoud, Gassi\ Touil, Nezla, Berkine,$

$RhoudNouss, Remote\ Operations\ Center\ (ROC),$

$Berkaoui, Ghardaya, Tindouf, North\ \ atlas\ Est,$

$North\ atlas\ Ouest\}$,

where

N is the nodes set which defines the regions,

E is the edges set which defines the road linking two different regions,

X is the edges weight which defines the numbers of hours separating two different regions, while traveling using Schlumberger cars and Schlumberger driving polices.

Heuristic: Problem solving

The heuristic that we defined is define based on the resources constraints that faces the logistic decision making process, in order to respond to the client requests in most efficient way.

We have been inspired by the shortest way algorithm and separate the graph in two sub trees in order to solve two sub mailman problems, using the heuristic defined below (Figure 16).

Failure Mode Effects Analysis

FMEA

Process Name: Relocation/NDJs job delivery Process
Process Number: RTOM-RS-01
Date: 05/01/2012 Revision Level: 1.0

FAILURE MODE	A) SEVERITY Rate 1-10 10=Most Severe	B) OCCURRENCE Probability Rate 1-10 10=Highest Probability	C) DETECTION Probability Rate 1-10 10=Lowest Probability	RISK PRIORITY NUMBER RPN AxBxC	ACTION TO IMPROVE	REVISED VALUES A	B	C	RPN
Lack Rig Support Resources (FIFO)	6	5	7	210	Study the work load and analyze need of resources	6	2	7	84
Missing Transportation (FIFO)	6	3	6	108	Study the work load and analyze need of transportation resources	6	2	6	72
Missing Drivers(FIFO)	6	2	6	72	Study the work load and analyze need of drivers	6	1	6	36
Process Not Followed	4	3	5	60	Improve jobs forecasting and communication plan between process actors	4	1	5	20
Planning process (FIFO)	6	6	6	216	Change way of thinking that feet the need and optimize the actual resources	6	3	6	108
Test Not Done	2	2	6	24	Test plan with all the services companies	2	1	6	12
HSE compliance	1	3	4	12	improve communication between security and RTOM team	1	3	4	12

Figure 11 – FEMA.

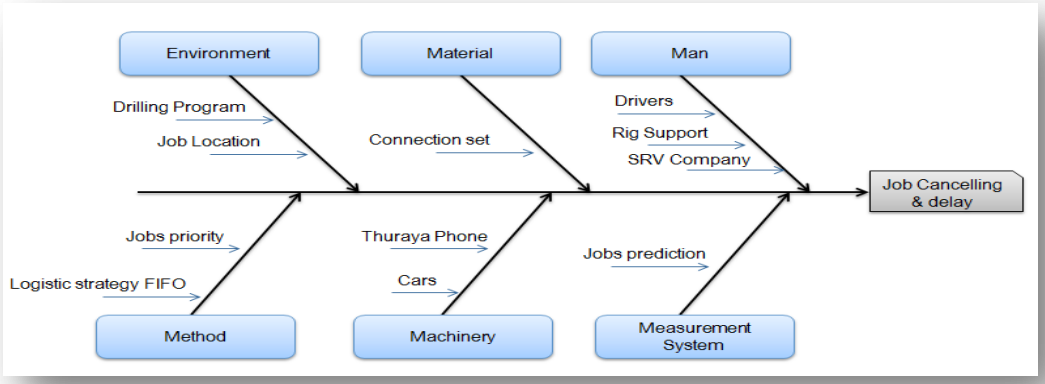

Figure 12 – Root Cause Analysis.

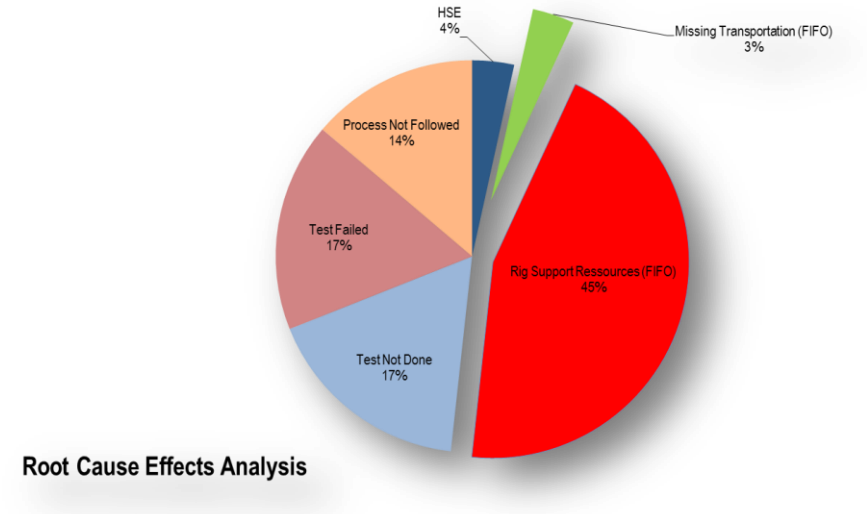

Figure 13 – Root Cause Effects Analysis.

Figure 14 – Algeria desert road network map.

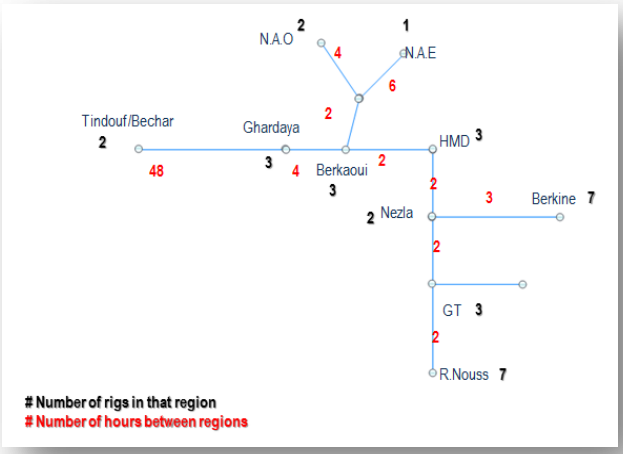

Figure 15 – Algeria desert road network, a graph representation.

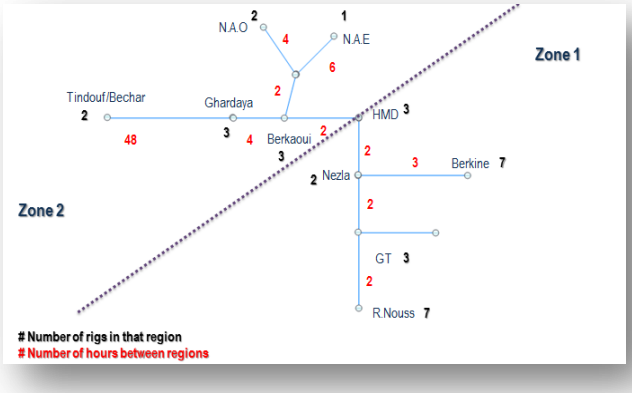

Figure 16 – Algeria desert road network, a separated graph representation.

Rig Support Job responds Heuristic

Step 1: Graph Separation:

Separate the graph in two sub trees as follow. We define the two sub trees as two main Zones: South HMD, and North HMD:

$G1 = \{N1, E1, X1\}$

$N1 = \{Hassi\ Messaoud, Gassi\ Touil, Nezla,$

$Berkine, RhoudNouss, (ROC)\}$

$G2 = \{N2, E2, X2\}$

$N2 = \{Berkaoui, Ghardaya, Tindouf,$

$North\ \ atlas\ Est, North\ atlas\ Ouest\}$

Step2: Resources Optimization:

The current resources constraints are:

- 5 Rig Support at any time
- 4 Cars (need 2 cars per trip → We can get only 2 trip at the same time)
- 4 Zones (2 accessible by cars, 2 by flight)

Based on these constraints we define the following rules:

- One trip per zone, we apply shortest way algorithm to minimize the path.
- The NDJ are prioritize on the relocations and deployment
- A deployment/ Relocation are done only and if there is no NDJ and we didn't pass the 5 days period after the well spud.
- If two jobs occur in the same zone at the same time we send two rig supports on the same convoy, we use the shortest way algorithm to minimize the path.

Step3: Cost Control and fatigue management:

As we have 5 rig support specialist per rotation at any time, and 5 Zone when we include the ROC as departure Zone in put in place the following rule in order to control the cost and manage the team fatigue, during the 5weeks (ON working).

We have notice that the risk of having defect in job delivery by the rig support is proportional to the time that he had spent ON working, for example if you send a rig specialist to the rig when it's his last week before going on days off, the risk of getting error while doing the job is higher due to cumulated fatigue during the last 5 weeks of nonstop work, this risk is also affected by the distance that separate the Rig from the ROC, thus will include other logistic constraint such as one flight per week between In Salah and Hassi Messaoud where the ROC is located.

Base on this analysis we get the following curves:

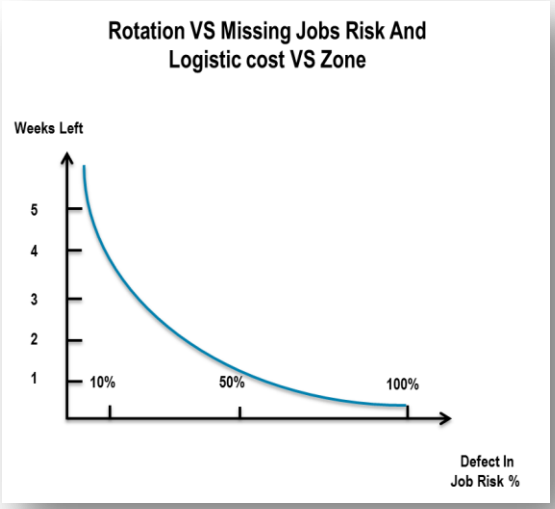

Figure 17 – Rotation vs. Missing Jobs Risk and Logistic cost vs. Zone

On the same way the cost analysis of the 4 Zones shows that In Salah is the highest cost Zone due to logistics constraints (1 flight per week, Hotel Booking, Cars renting to move between the rigs), based on all this constraints we get the following Histogram:

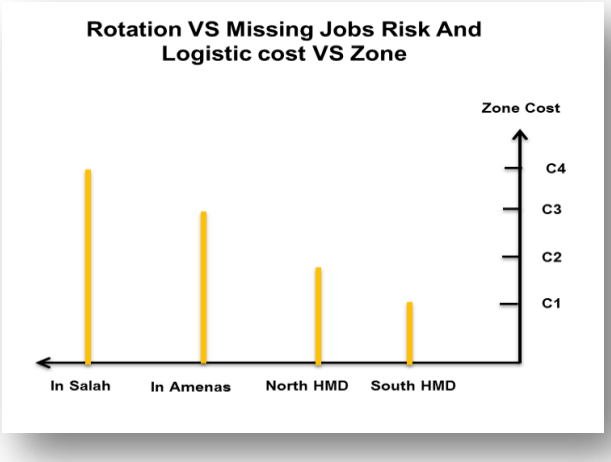

Figure 18 – Rotation vs. Missing Jobs Risk and Logistic cost vs. Zone Diagram

By Doing a simple comparison between the two analyses we get the following zone assigning rule (Figure 19):

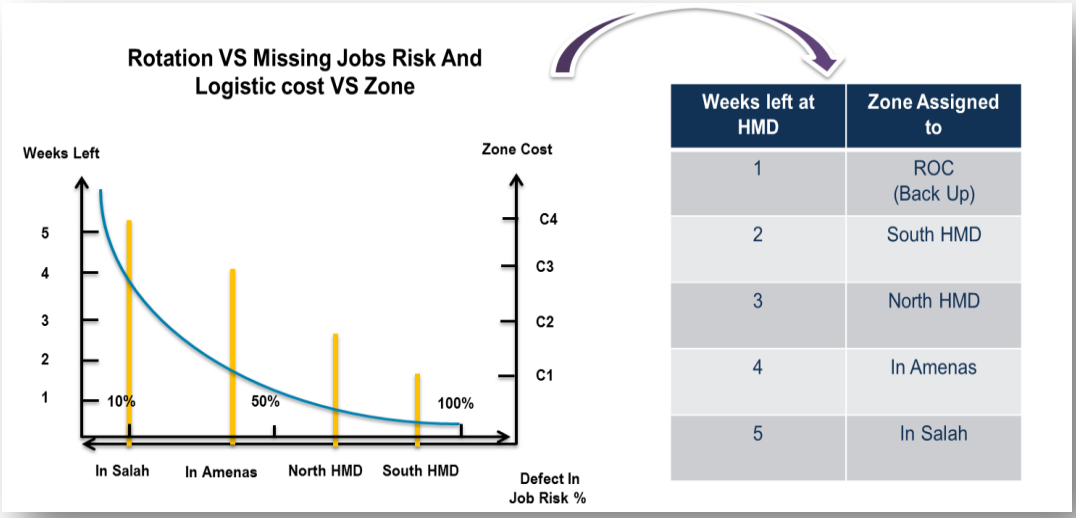

Figure 19 – Rotation vs. Missing Jobs Risk and Logistic cost vs. Zone Rule

These two analyses lead us to say that for the people whom just came from days off they will be assigned to the jobs in In-Salah (the farther location), and so on until they reach the last week where they will be assigned to the ROC as backup resource and help desk tasks.

By minimizing the risk of having defect on job delivery we will avoid extra cost in trying to fix error on jobs execution.

By avoiding sending people to far location at the end of their rotation this will help us to manage their fatigue and getting best performance from them while job execution.

These two rules will lead us to reduce the cost of red money, and also manage the team performance.

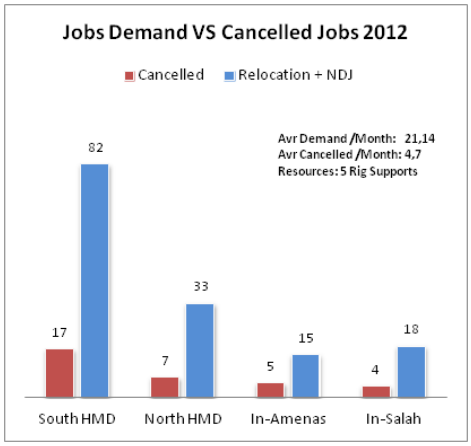

Figure 20 – Jobs Demand VS Cancelled Jobs (2012).

2012 statistic and control plan

Since we applied this heuristic starting April 2012, we observed a huge changes and impact on our performance and revenue, the matrixes below show our 2012 performance (Figure 21, Figure 22). NB: This matrix has been put in place July 2012. In 2012 we get a pick in the client job demand 21.14 jobs/month comparing to 2011 where we were having only 15.4 jobs/month. We still cancelling 4,7 job/month, but none of the cancelling root causes is due to lack of resources or logistic management system, and the most important point is using this new logistic method our capacity of job responds is 30jobs/month by adding only one resource comparing to 2011 where we were having 4 rig supports specialists.

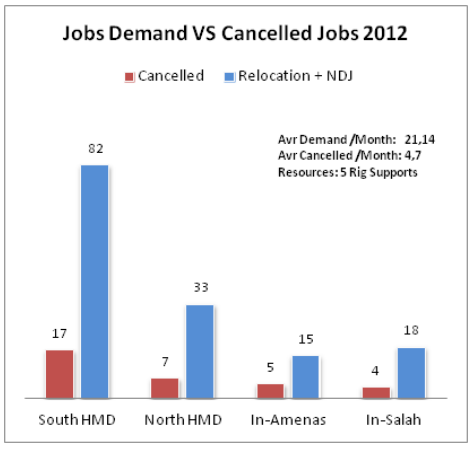

Figure 21 – Jobs Demand VS Cancelled Jobs (2012).

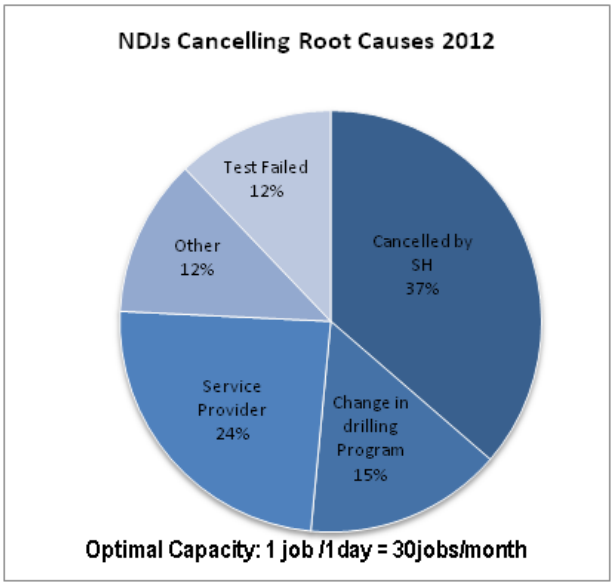

Figure 22 – NDJs Cancelling Root Causes (2012).

These changes had a direct impact on our cost, in fact we realized $241K as hard saving in 2012, and total of $503k of saving when we include the soft saving such as time saving and job quality delivery.

The unit job cost decline from $1004.52.to $844.82 per job. Those performances raised the sigma level of the RTOM job delivery from 2.5 **b** to 3.1 **b**.

Below is the summary of 2012 performances (All the year).

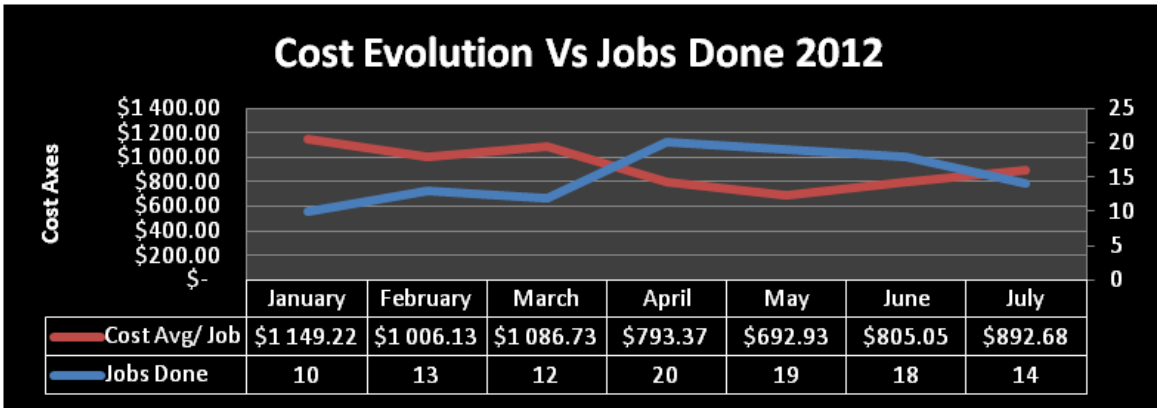

Figure 23 – Cost Evolution Vs Jobs Done (2012).

	2011	2012
Total Cost	$ 126,569.06	$ 160,515.70
Cost/ Job Avr	$ 1,004.52	$ 844.82
Total Jobs Done	126	190
Rig Support Numbers	6	8
Cars Number	4	4
Drivers number	2	4

Figure 24 – Summary of 2012 performances (All the year).

Methodology to Select a Production Riser to Reduce Heat Transfer and Prevent Formation of Hydrates and Precipitation of Waxes and Paraffins

Alejandro Cortés Cortés, Well Engineer, IPM Well Constructions, Rio de Janeiro, Brasil

Ascencio Cendejas, National Autonomous University of Mexico-Petroleos Mexicanos

Abstract

This work presents the mathematical approach to develop the equation that defines the temperature variation for convective heat transfer. Considerations over steady state and unsteady state regimen were performed. The methodology used involves the general energy balance equation and viscosity equation for temperature variation (Arrhenius´s equation). The results obtained show that the affectation level under free convection behavior, greatly affects the oil viscosity that flows through a production riser system installed at 500 mts (1640 ft) of deepwater. A representative behavior of the oil viscosity flowing along the production riser was determined.

Introduction

The exploitation of hydrocarbons in deepwater is a technology and scientific challenge because en subsea environments, but most in water columns over 200 m (656 ft), are presented flow assurance problems. In the production engineering area, is essential the knowledge of the temperature along the pipe, due to its importance on the hydrocarbon viscosity.

A fluid at a high temperature flowing through a system at a lower temperature, suffers physic and chemical structure changes, like the viscosity raise level, which is caused by the temperature decrease. Increasing oil viscosity through time under those conditions, the lines and separators can be plugged when paraffin or hydrates are formed generating pressure and production losses, affecting the productivity of the well.

The object of this paper is to derivate the equations that defines the viscosity behavior with temperature variation. Afterward evaluate the equation for several flow rates conditions, oil properties and analyze the results.

Background

To understand the development of this work is important to understand the Heat Transfer modes by Conduction and Convection, both evolved in Fourier´s Law. Through

Thermal Conduction

The conduction is carried out by means of the energy transference between adjacent molecules and have place every time there is a temperature gradient.

Materials have a main parameter that regulates the temperature, and that is thermal conductivity “k”. Fourier’s law says that the heat flow is directly proportional to a thermal constant named “k”, temperature differential and is inversely proportional to the differential of length and a sectional area of flow.

$$\frac{dQ_x}{dt} = -kA\frac{\partial T}{\partial x} \qquad (1)$$

Thermal Convection

Convection is the mode of transfer of heat from one place to another by the massive movement of fluids. Contrary to conduction, convection exists in the movement of big fluid volumes.

Convection heat transference means the heat transportation through a phase and the mixture of hot and cold liquid or gas proportions. If the movement of the fluid is generated in a natural convection; if this movement is assisted by any external flurry, it is named forced convection. In fluids the heat transmission by conduction is practically despicable compared to the one obtained by convection.

Convective heat transmission of a fluid in contact with a hot surface is expressed in the by

$$q = hA(T_p - T_f) \qquad (2)$$

where

q: is thermal energy (per time).

h: is heat transfer coefficient.

A: is the surface area of the heat being transferred.

Tf: fluid temperature (hydrocarbons).

Tp: is the surface temperature (pipe).

Using the energy balance equation was performed the equation used to solve this work, considering that the effects of viscosity dissipation are negligible in r y θ then the

$$\left\{\begin{matrix}\text{Rate of heat in}\\ \text{through a circular surface}\\ z\end{matrix}\right\}-\left\{\begin{matrix}\text{Rate of heat out}\\ \text{through a circular surface}\\ z+\Delta z\end{matrix}\right\}-\left\{\begin{matrix}\text{Rate of heat lost}\\ \text{by convection}\\ \text{to the exterior}\end{matrix}\right\}=0,$$

Appendix A shows the development of this equation.

Case I "Steady-state"

Considering flow in z direction, the final equation derived from the mathematical approach to model the temperature behavior is represented by

$$\Delta T = \Delta\bar{T}\left(1-e^{-\frac{2hz}{\lambda}}\right), \qquad (3)$$

where

ΔT : *Temperature variation.*

$\Delta\bar{T}$: *Differential convective of temperature.*

λ : *dimensionless variable* $\lambda = \frac{2h}{\rho_f C_f R v_z}$

h : *heat convection coefficient.*

z : *depth.*

Case II "Unsteady-state"

Carried out an analyzis of our control volume element and considering our flow in Z direction is function of the time, the equation derived from this mathematical approach and that represents the temperature profile is the next equation (4)

$$\Delta T = \frac{\Delta T}{e^{\lambda k v_z}} * u\left(t+\frac{z}{v_z}\right), \qquad (4)$$

where

ΔT : *Temperature variation.*

$\Delta\bar{T}$: *Differential convective of temperature.*

λ : *dimensionless variable* $\lambda = \frac{2U_o}{\rho_f C_f R v_z}$

Uo : *Global coefficient of transfer.*

z : *depth.*

$u\left(t+\frac{z}{v_z}\right)$: *Heaviside´s function.*

k : *Variable* z/v_z

Viscous Fluids

From mechanics of fluids, is knows that the change of the viscosity in a fluid is consequence of 4 physical effects:

- Deformation rate,
- Exposition time to the shear stress,
- Temperature y finally,
- Pressure.

For the mathematical approach in this paper were used the equations that define the change in the viscosity due to the temperature variation, and the results obtained were compared, to find which behavior show a real behavior of the fluid.

Arrhenius´s equation is:

$$\mu = Ae^{-B/T}, \qquad (5)$$

where

T: *Absolute temperature of the equation.*

A y B: *Material constant to analyze*

Development of the problem

The approach of the problem starts with some considerations addressed below.

Suppose a well located in offshore environment, to 500 m of deepwater, producing oil at 80°C and 200 cp of viscosity when it arrives to the mudline. The flow in the production riser, is interacting with the system where the water temperature is 10ºC, and for that reason the viscosity increase to 5000 cp.

The following considerations are:

- Temperature gradient of the water is negligible; water temperature is 10 (ºC).
- Oil properties:
- Cpoil =1900(J/(kg°C)),
- Koil =0.3(W/(m°C))
- Inside Diameter production tubing =2.992(pg)
- Density of the oil is constant.
- The effects of the heat transfer by conduction are negligible for the steady state.
- Gravity effects are negligible.

- Upstream flow in Z direction.
- Steady state for the first case.
- Unsteady state for the second case.

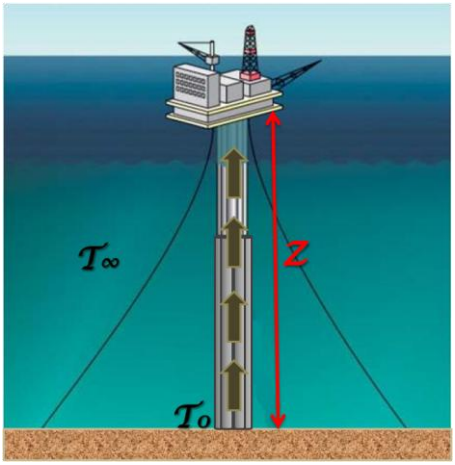

Figure 25 – Conditions for a well located in offshore environment

Steady State

Therefore the temperature behavior along the riser in steady state is defined by the equation:

$$\Delta T = \Delta \bar{T}\left(1-e^{-\frac{2hz}{\lambda}}\right)$$

considering the next boundary conditions:

$$z = 0 \rightarrow T = T_0$$

$$T(z,T) = T_\infty$$

To solve the equation is necessary use an iterative method that meets the following algorithm:

1. Viscosity computation through the Arrhenius equation:

$$\mu = Ae^{-B/T}$$

where

$$A = 7149.64, B = 0.035765\ y\ T = T_0$$

2. Reynolds number computation:

$$Re = \frac{\rho v D}{\mu}$$

where

$$v = \frac{q}{A} = \frac{1.84 \times 10^{-4}\left(\frac{m^3}{s}\right)}{\pi(0.038m)^2} = 0.0405\left(\frac{m}{s}\right)$$

3. Prant number computation:

$$p_r = \frac{\mu c_p}{k}$$

4. Nusell number computation:

$$N_u = 1.86\left(\frac{Rep_r D}{L}\right)^{1/3}\left(\frac{\mu_b}{\mu_s}\right)^{0.14}$$

where

$$L = 50(m)$$

$$\mu_b: viscosity\ that\ change\ with\ the\ temperature$$

$$\mu_s: viscosity\ at\ surface\ conditions\ @\ 10°C$$

5. Coefficient of thermal transmission

$$h = \frac{N_u k}{D}$$

6. determination of ΔT:

$$\Delta T = \Delta \bar{T}\left(1-e^{-\frac{2hz}{\lambda}}\right)$$

where

$$\Delta \bar{T} = T_0 - T_\infty = 80(°C) - 10(°C) = 70(°C)$$

$$\lambda = \rho C_p R v$$

$$z: position\ where\ is\ measure, z = z + L$$

7. Determination of T:

$$T = \Delta T + T_0$$

8. Calculation of corrected viscosity with Arrhenius Equation with the temperature value in step 7

9. Repeat steps 2 to 8 until the desired tolerance is met for the viscosity value.

Unsteady state

For the unsteady state regime, the equation that defines the behavior of the temperature profile along the riser is:

$$\Delta T = \frac{\overline{\Delta T}}{e^{\lambda k v_z}} * u\left(t + \frac{z}{v_z}\right)$$

with the following boundary conditions:

$$T(z\,, t = 0) = T_\infty$$

$$T(z = 0\,, t) = T_0$$

1. To solve the equation, was used the heat transfer coefficient, defined for the above problem therefore was repeated from step 1 to 5.

2. It is proposed to design a production riser formed with different materials, each material with a thermal

conductivity property, then the analysis was carried out as follows:

The design of the riser was analyzed with the following materials

- Steel.
- Brine.
- Steel.
- Shell of the riser.
- Sea water to steady conditions.

Assumptions:

- The oil flow inside transmit heat by convection due to its speed.
- The components of a, b, c, d and e transmit heat by conduction. Analyzing a cross-section of the riser, the following defined radios and materials:
-

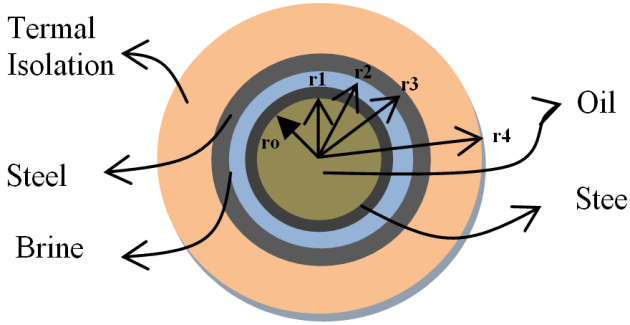

Figure 26 – Heat transmission, components a…e.

6 cases were proposed, in which the packer fluid in the riser was changed for different liquids:

- Brine of NaCl, 80,000 ppm a 10 °C.
- Diesel.
- Air.
- Brine of NaCl, 80,000 ppm a 10 °C with no thermal isolation material.
- Diesel with no thermal isolation material.
- Air with thermal isolation material.

Then the equation to define the global coefficient is:

where:

ro= 0.036 mm IR of the TP(Steel).

r1= 0.0437 mmOR of the TP (Steel).

r2= 0.106 mmIR of the Riser (Steel)

r3= 0.1203 mmOR of the riser (Steel)

r4= 0.2 mmOR of the isolation (synthetic foam)

3. Heat transfer coefficient values were estimated in Section 5, to calculate the global coefficient for each L = 50 (m), accumulated.

4. Calculus of ΔT:

$$\Delta T = \frac{\overline{\Delta T}}{e^{\lambda k v_z}} * u\left(t + \frac{z}{v_z}\right)$$

where:

$$\Delta \bar{T} = T_0 - T_\infty = 80(°C) - 10(°C) = 70(°C)$$

$$\lambda = \frac{2U_0}{\rho_f C_f R v_z}$$

$$z: position\ where\ is\ measure, z = z + L$$

5. Calculus of T:

$$T = \Delta T + T_0$$

6. Calculation of corrected viscosity using Arrhenius Equation with the temperature value in step 3.

Results and discussions

Graphical and numerical comparisons of the degree of involvement of temperature on the viscosity were obtained. With equations 4 and 5, the profiles of viscosity change as a function of temperature were obtained.

In Figure 28 it can be seen, that the change in viscosity is a function of the fluid velocity as mentioned above.

The degree of change in viscosity is different from equations 4 and 5. The expression 5 shows a better profile of the distribution as shown in Figure 30, for different production rates.

Conclutions

Steady State:

The flow rate influences inversely proportional to the heat loss from the fluid. Figures 27 and 29 shows that as the rate increase, temperature decrease at the same height; this is because with the increment of the flow exist a increment of the velocity and therefore a reduction in the residence time of the fluid in the low temperature system.

In the same way, when the production flow increase, the increment of the viscosity, due to the change of the temperature, decrease along of the trajectory of the fluid.

For the unsteady state, is observed that the equation that represents the behavior is not dependent of the time, only of the velocity.

Figure 29 and 30 of the Appendix B show, that the heat isolation material with better performance are the diesel and brine in the riser involved with synthetic foam. The variation of the temperature obtained in both cases is (0.003 °C each 50 m).

According to the cost of the brain to 80,000 pm and at 10°C is economically better that the use of diesel due to the transportation on the sea.

The equation to define the variation of the temperature for unsteady-state regime, have a numerical limitation for velocities below of 150 BPD, because were presented trivial solutions.

Appendix A. Development of the Temperature and Viscosity equation

Is necessary predict the velocity and viscosity behavior of an oil transported from the mudline to the surface through a 3.5 in production tubing of outside diameter and a length of 500m. The oil production is 100 BPD, with 80°C of temperature at the mudline level.

The first case, steady state requires a control volume to facilitate the analysis

$$\left\{\begin{matrix}Rate\ of\ heat\ in\\ through\ a\ circular\ surface\\ z\end{matrix}\right\}-\left\{\begin{matrix}Rate\ of\ \ heat\ out\\ through\ a\ circular\ surface\\ z+\Delta z\end{matrix}\right\}-\left\{\begin{matrix}Rate\ of\ heat\ lost\\ by\ convection\\ to\ the\ exterior\end{matrix}\right\}=0$$

$$\left\{\pi R^2\rho C_p v_z T\big|_z\right\}-\left\{\pi R^2\rho C_p v_z T\big|_{z+\Delta z}\right\}-\{2\pi R\Delta z h(T-T_\infty)\}=0$$

Dividing all terms by $\pi R^2\rho C_p v_z \Delta z$:

$$\frac{T|_z - T|_{z+\Delta z}}{\Delta z}-\frac{2h(T-T_\infty)}{R\rho C_p v_z}=0$$

Applying the limit when $\Delta z \to 0$:

$$\frac{dT}{dz}-\frac{2h}{R\rho C_p v_z}(T-T_\infty)=0$$

Defining:

$$\lambda=\frac{2h}{R\rho C_p v_z}$$

$$\Delta T = T_0 - T$$

$$\Delta\bar{T} = T_0 - T_\infty$$

Replacing; the differential equation results:

$$\frac{d\Delta T}{dz}=-\frac{2h}{\lambda}(\Delta T-\Delta\bar{T})$$

with the boundary condition:

$$z=0\ \to T=T_0$$

grouping variables as follows:

$$\frac{d\Delta T}{(\Delta T-\Delta\bar{T})}=-\frac{2h}{\lambda}dz$$

Integrating both sides:

$$\int\frac{d\Delta T}{(\Delta T-\Delta\bar{T})}=-\int\frac{2h}{\lambda}dz$$

$$Ln(\Delta T-\Delta\bar{T})=-\frac{2hz}{\lambda}+C_1$$

clearing ΔT

$$e^{Ln(\Delta T-\Delta\bar{T})}=e^{-\frac{2hz}{\lambda}+C_1}$$

$$\Delta T-\Delta\bar{T}=e^{-\frac{2hz}{\lambda}}e^{C_1}$$

$$\Delta T-\Delta\bar{T}=\frac{e^{C_1}}{e^{\frac{2hz}{\lambda}}}$$

$$\Delta T=\frac{e^{C_1}}{e^{\frac{2hz}{\lambda}}}+\Delta\bar{T}$$

$$\Delta T=\frac{C_1}{e^{\frac{2hz}{\lambda}}}+\Delta\bar{T}$$

when

$$\Delta T = T_0 - T$$

$$\Delta\bar{T} = T_0 - T_\infty$$

Applying the boundary condition $T(z=0\,,T)=T_0$

$$\Delta T=\frac{C_1}{e^{\frac{2h(0)}{\lambda}}}+\Delta\bar{T}$$

$$\Delta T = C_1+\Delta\bar{T}$$

$$T_0 - T_0 = C_1+(T_0-T_\infty)$$

$$0 = C_1+(T_0-T_\infty)$$

$$C_1=-(T_0-T_\infty)$$

$$C_1=-\Delta\bar{T}$$

replacing ΔT in equation:

$$\Delta T=\frac{-\Delta\bar{T}}{e^{\frac{2hz}{\lambda}}}+\Delta\bar{T}$$

$$\Delta T=-\Delta\bar{T}e^{-\frac{2hz}{\lambda}}+\Delta\bar{T}$$

Finally

$$\Delta T = \Delta \bar{T}\left(1-e^{-\frac{2hz}{\lambda}}\right)$$

To solve the previous equation is necessary use an iterative method that meets the next algorithm

1. Calculation of viscosity with Arrhenius equation:

$$\mu = Ae^{-BT}$$

where:

$$A = 7149.64, B = 0.035765\ y\ T = T_0$$

2. Calculation with the Reynolds number:

$$Re = \frac{\rho v D}{\mu}$$

where

$$v = \frac{q}{A} = \frac{1.84 \times 10^{-4}\left(\frac{m^3}{s}\right)}{\pi(0.038m)^2} = 0.0405\left(\frac{m}{s}\right)$$

3. Calculation of the Prant number:

$$p_r = \frac{\mu c_p}{k}$$

4. Calculation of the Nusell number:

$$N_u = 1.86\left(\frac{Rep_r D}{L}\right)^{1/3}\left(\frac{\mu_b}{\mu_s}\right)^{0.14}$$

where

$$L = 50(m)$$

μ_b: $viscosity\ that\ varies\ with\ the\ temperature$

μ_s: $surface\ viscosity\ @\ 10°C$

5. calculation of the thermal transfer coefficient.

$$h = \frac{N_u k}{D}$$

6. Calculating ΔT:

$$\Delta T = \Delta \bar{T}\left(1-e^{-\frac{2hz}{\lambda}}\right)$$

where

$$\Delta \bar{T} = T_0 - T_\infty = 80(°C) - 10(°C) = 70(°C)$$

$$\lambda = \rho C_p R v$$

z: $position\ where\ is\ measure, z = z + L$

7. Calculating of T:

$$T = \Delta T + T_0$$

8. Calculation of corrected viscosity with Arrhenius equation using the temperature value calculated in step 7.

9. Repeat steps 2 to 8 until the desired tolerance comply for the viscosity value.

$$q = hA(T_p - T_o)$$

Unsteady-State

For the second case, involves analyzing the control volume, including the time as follows.

$$\frac{\partial T}{\partial z} - \frac{2U_0}{\rho_f C_f R}(T_0 - T_\infty) = \frac{\partial T}{\partial t}$$

Multiplying equation number (4) by $1/v_z$, the equation is reduced to the next expression:

$$\frac{v_z}{v_z}\frac{\partial T}{\partial z} - \frac{2U_0}{\rho_f C_f R v_z}(T_0 - T_\infty) = \frac{1}{v_z}\frac{\partial T}{\partial t}$$

Reducing terms and proposing a change of variable, where $\lambda = \frac{2U_0}{\rho_f C_f R v_z}$ y $\Delta T = (T_0 - T_\infty)$, the equation can be reduced to:

$$\frac{\partial \Delta T}{\partial z} - \lambda \Delta T = \frac{1}{v_z}\frac{\partial \Delta T}{\partial t}$$

Applying Laplace Transform to the preview equation and using the boundary conditions:

$$\mathfrak{L}\left\{\frac{\partial \Delta T}{\partial z}\right\} - \mathfrak{L}\{\lambda \Delta T\} = \frac{1}{v_z}\mathfrak{L}\left\{\frac{\partial \Delta T}{\partial t}\right\}$$

$$\mathfrak{L}\{T(z, t=0)\} = 0$$

$$\mathfrak{L}\{T(z=0, t)\} = \frac{\overline{\Delta T}}{s}$$

Applying derivative operator in Laplace space and the initial condition, becomes:

$$\frac{d\overline{\Delta T}}{dz} - \lambda \overline{\Delta T} = \frac{\overline{\Delta T}}{s v_z}$$

Rearranging the previous equation and using to ΔT as common factor, thus:

$$\frac{d\overline{\Delta T}}{dz} = \overline{\Delta T}\left(\frac{s}{v_z} + \lambda\right)$$

Solving the preview differential equation through the next procedure:

$$\int \frac{d\overline{\Delta T}}{\overline{\Delta T}} = \left(\frac{s}{v_z} + \lambda\right)\int dz$$

where the solution is

$$\ln \overline{\Delta T} = \left(\frac{s}{v_z} + \lambda\right) z + C_1$$

Applying the properties of the exponential, the equation become as:

$$\overline{\Delta T} = e^{\left(\frac{s}{v_z}+\lambda\right)z+C_1}$$

As per the exponent properties, is obtained:

$$\overline{\Delta T} = e^{\left(\frac{s}{v_z}+\lambda\right)z} \cdot C_1$$

Evaluating the preview equation with the boundary condition, the next expression is generated:

$$C_{1=}\frac{\overline{\Delta T}}{s}$$

Replacing C_1 in the general equation, we have:

$$\Delta T = \frac{\overline{\Delta T}}{s} e^{\left(\frac{s}{v_z}+\lambda\right)z}$$

Proposing a change of variable $k = \frac{z}{v_z}$ and replace it in the preview equation, is obtained:

$$\Delta T = \frac{\overline{\Delta T}}{s} e^{(sk-\lambda k v_z)}$$

Applying the rule of the exponent, the preview equation become in:

$$\Delta T = \frac{\overline{\Delta T}}{s} \frac{e^{(sk)}}{e^{\lambda k v_z}}$$

Where the term $1/e^{\lambda k v_z}$ is not in Laplace space, therefore is a constant, then:

$$\Delta T = \frac{1}{e^{\lambda k v_z}} \cdot \frac{\overline{\Delta T}}{s} \cdot e^{(sk)}$$

From the "Handbook of Mathematical Functions" of Abramowits Stegun, page 1025, equation 29.3.61 the solution that describe the solution in the real space is

$$\frac{1}{s} e^{-ks} \longrightarrow u(t+k)$$

This equation represents the Heaviside unit step function. In the approach of this problem, the function was assessed in Mathematica 8.0, was deduced that for times greater than zero, our sample argument values is equal to 1, showing that numerically varying the viscosity does not depend on time, depends only on the exponent. Therefore the general equation defining the variation of the temperature is

$$\Delta T = \frac{\overline{\Delta T}}{e^{\lambda k v_z}} \cdot u\left(t + \frac{z}{v_z}\right)$$

Appendix B. Results obtained with Arrhenius equation

For this case, iterations of the viscosity were performed under the assumptions of the problem, obtaining the following results:

Table 3 - Results of the variation of the viscosity using Arrhenius equation

z	q= 100 [BPD]		q= 500 [BPD]		q= 1000 [BPD]	
	T	μ	T	μ	T	μ
[m]	[C]	[Pa*s]	[C]	[Pa*s]	[C]	[Pa*s]
500	10.0312	4.9470	18.7643	0.9410	31.4813	0.4357
450	10.0683	4.8823	21.4449	0.7415	34.5269	0.3941
400	10.1517	4.7419	24.6581	0.5966	37.8805	0.3596
350	10.3456	4.4389	28.4582	0.4916	41.5700	0.3307
300	10.8346	3.7975	32.9150	0.4146	45.6271	0.3063
250	12.1855	2.6336	38.1169	0.3575	50.0873	0.2857
200	15.5857	1.3881	44.1731	0.3143	54.9905	0.2680
150	22.3397	0.6936	51.2158	0.2812	60.3811	0.2529
100	33.7431	0.4037	59.4033	0.2554	66.3085	0.2399
50	51.7852	0.2790	68.9226	0.2350	72.8276	0.2286

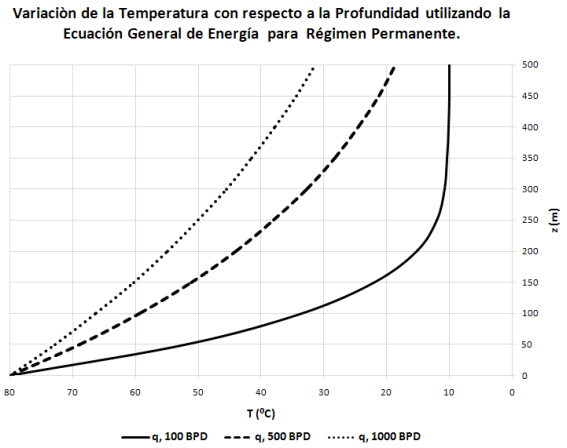

Figure 27 – Variation of the temperature according to the depth

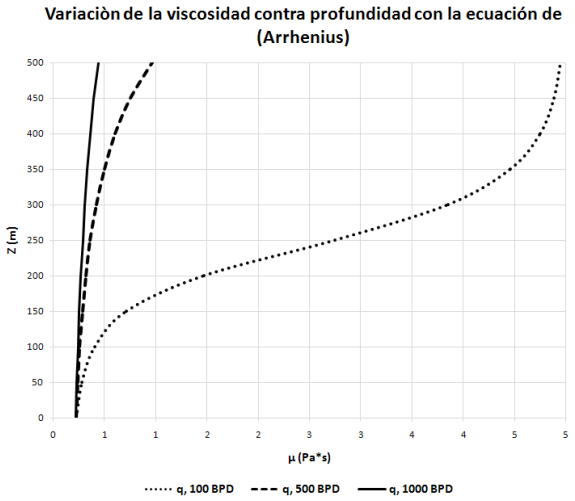

Figure 28 – Variation of the viscosity according to the depth

Transient regime

The next tables show the results obtained to different rates and conditions according to the assumptions described in this work.

Table 4 - Variation of the viscosity using the Arrhenius equation when brine is between the annular apace of the riser and tubing

	Salmuera en el Riser					
	q= 100 [BPD]		q= 500 [BPD]		q= 1000 [BPD]	
z	T	μ	T	μ	T	μ
[m]	[C]	[Pa*s]	[C]	[Pa*s]	[C]	[Pa*s]
500	10.1203	4.7940	10.0331	4.9435	10.0182	4.9699
450	10.1081	4.8145	10.0291	4.9507	10.0161	4.9736
400	10.0958	4.8353	10.0251	4.9576	10.0141	4.9772
350	10.0832	4.8567	10.0214	4.9642	10.0121	4.9806
300	10.0703	4.8789	10.0178	4.9705	10.0103	4.9840
250	10.0569	4.9020	10.0145	4.9764	10.0084	4.9872
200	10.0433	4.9257	10.0113	4.9821	10.0067	4.9904
150	10.0301	4.9488	10.0083	4.9874	10.0049	4.9934
100	10.0184	4.9694	10.0054	4.9926	10.0033	4.9964
50	10.0084	4.9873	10.0027	4.9975	10.0016	4.9994

Table 5 - Variation of the viscosity using the Arrhenius equation when diesel is between the annular space of the riser and tubing

	Diesel en el Riser					
	q= 100 [BPD]		q= 500 [BPD]		q= 1000 [BPD]	
z	T	μ	T	μ	T	μ
[m]	[C]	[Pa*s]	[C]	[Pa*s]	[C]	[Pa*s]
500	10.121909	4.7913155	10.0284909	4.95166764	10.015426	4.97476066
450	10.109549	4.81206157	10.0250841	4.9576732	10.0136899	4.9778419
400	10.0970483	4.83318713	10.02178	4.96350859	10.0120043	4.98083647
350	10.0843079	4.85486756	10.0186019	4.9691316	10.0103678	4.98374649
300	10.0711987	4.87733481	10.0155647	4.97451458	10.0087779	4.98657616
250	10.0576388	4.90074576	10.0126732	4.97964792	10.0072313	4.98933126
200	10.0438202	4.92478459	10.009922	4.98453977	10.0057239	4.99201872
150	10.030478	4.94816989	10.0072979	4.98921255	10.0042514	4.99464609
100	10.0186235	4.96909341	10.0047828	4.99369767	10.0028095	4.99722111
50	10.0084595	4.98714324	10.002346	4.9980492	10.0013901	4.99975779

Table 6 - Variation of the viscosity using Arrhenius equation when there is no liquid in the annular space of the riser and the tubing (only exist air)

	Vacio en el Riser					
	q= 100 [BPD]		q= 500 [BPD]		q= 1000 [BPD]	
z	T	μ	T	μ	T	μ
[m]	[C]	[Pa*s]	[C]	[Pa*s]	[C]	[Pa*s]
500	9.42431392	6.22384818	9.95017017	5.09265871	9.97800808	5.04183696
450	9.47868932	6.0897994	9.95333274	5.08684497	9.9797989	5.03859465
400	9.5299624	5.96740248	9.95659347	5.08086157	9.98167162	5.03520753
350	9.57524218	5.86241944	9.96006093	5.07451084	9.98363398	5.03166209
300	9.60873313	5.78658209	9.9638646	5.06755855	9.98569135	5.02794917
250	9.61196946	5.77933369	9.96814352	5.0597553	9.98784641	5.02406452
200	9.73793424	5.5077176	9.97302906	5.05086865	9.99009908	5.02000893
150	5.45636783	98.3497222	9.97862499	5.04071967	9.99244663	5.01578794
100	10.2481484	4.58721576	9.98499042	5.02921366	9.99488406	5.0114112
50	10.0530831	4.90865066	9.99200948	5.01657354	9.99739206	5.00691395

Table 7 - Variation viscosity using Arrhenius equation when diesel is in the annular between the riser and tubing, but there is no external insulating around the riser

	Diesel en el Espacio Anular sin Recubrimiento en el Riser					
	q= 100 [BPD]		q= 500 [BPD]		q= 1000 [BPD]	
z	T	μ	T	μ	T	μ
[m]	[C]	[Pa*s]	[C]	[Pa*s]	[C]	[Pa*s]
500	10.1307303	4.77659454	10.037203	4.93636124	10.0206682	4.96547451
450	10.1174625	4.79876275	10.0325386	4.94454698	10.018256	4.96974429
400	10.1040329	4.8213656	10.0280597	4.95242705	10.0159364	4.97385532
350	10.0903283	4.84460366	10.0238016	4.95993691	10.0137058	4.9778137
300	10.0762022	4.86874037	10.019784	4.9670389	10.0115586	4.98162886
250	10.0615657	4.89394801	10.0160093	4.97372608	10.0094876	4.98531271
200	10.0466479	4.9198506	10.0124639	4.98001981	10.0074852	4.98887871
150	10.0322937	4.94497737	10.0091225	4.98596269	10.0055432	4.99234102
100	10.0196355	4.96730178	10.0059534	4.99160942	10.0036534	4.99571379
50	10.0088751	4.98640321	10.0029067	4.99704746	10.001802	4.99902137

Table 8 - Variation of the viscosity using Arrhenius equation when brain is in the annular of the riser and tubing, but there is no external isolating

	Salmuera en el Espacio Anular sin Recubrimiento en el Riser					
	q= 100 [BPD]		q= 500 [BPD]		q= 1000 [BPD]	
z	T	μ	T	μ	T	μ
[m]	[C]	[Pa*s]	[C]	[Pa*s]	[C]	[Pa*s]
500	10.1326215	4.77344772	10.0314596	4.94644346	10.0171821	4.97164684
450	10.1191588	4.79591949	10.0276354	4.95317467	10.0152243	4.97511845
400	10.1055297	4.81883819	10.0239389	4.95969454	10.0133296	4.9784818
350	10.0916177	4.84240998	10.0203975	4.96595338	10.011496	4.98174004
300	10.0772724	4.86690526	10.0170281	4.97191983	10.0097202	4.98489883
250	10.0624035	4.89249956	10.0138349	4.97758453	10.0079977	4.98796569
200	10.0472488	4.91880317	10.0108103	4.98295933	10.0063235	4.99094947
150	10.0326773	4.94430322	10.0079376	4.98807272	10.004692	4.99385969
100	10.0198481	4.9669256	10.0051944	4.99296333	10.0030978	4.99670602
50	10.0089618	4.98624873	10.0025437	4.99769591	10.0015311	4.99950564

Table 9 - Variation of the viscosity using Arrhenius equation when no liquid is in the annular of the riser and tubing, and external isolating material is around the riser

	Vacio en Espacio Anular sin Recubrimiento en el Riser					
	q= 100 [BPD]		q= 500 [BPD]		q= 1000 [BPD]	
z	T	μ	T	μ	T	μ
[m]	[C]	[Pa*s]	[C]	[Pa*s]	[C]	[Pa*s]
500	9.07036389	7.21743118	9.65881696	5.67595447	9.97425772	5.04863759
450	9.15581486	6.95661822	9.68581689	5.6176609	9.97627026	5.04498641
400	9.23347604	6.73174225	9.70874355	5.56888294	9.97839178	5.04114199
350	9.29574185	6.55930773	9.72480267	5.53510412	9.98063413	5.03708355
300	9.31566201	6.50555674	9.72951727	5.52524745	9.98300619	5.03279591
250	9.50033595	6.03766082	9.64737263	5.70094466	9.98551321	5.02827049
200	5.65995684	77.6897107	11.5976407	3.05608481	9.98815664	5.0235057
150	10.5144707	4.19907738	45.720816	0.30582068	9.99093414	5.01850683
100	10.1363006	4.76733531	10.2258734	4.62222572	9.99383994	5.01328533
50	10.0392701	4.93274035	10.0531727	4.90849494	9.99684723	5.00789038

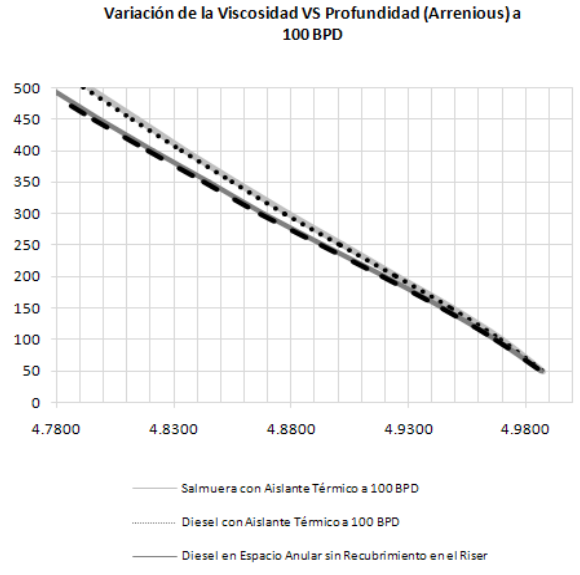

Figure 29 – Behavior of the well producing at 100 BPD when different fluids are in the annular and there exists an insulating material around the riser

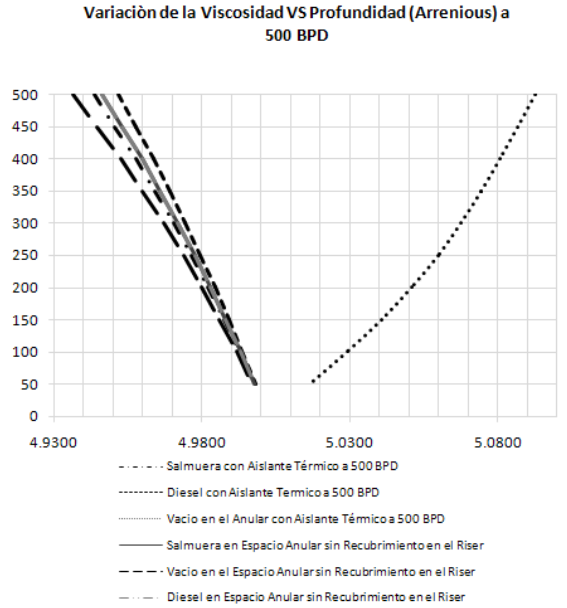

Figure 30 – Behavior of the well producing at 500 BPD when different fluids are in the annular and there exists an insulating material around the riser

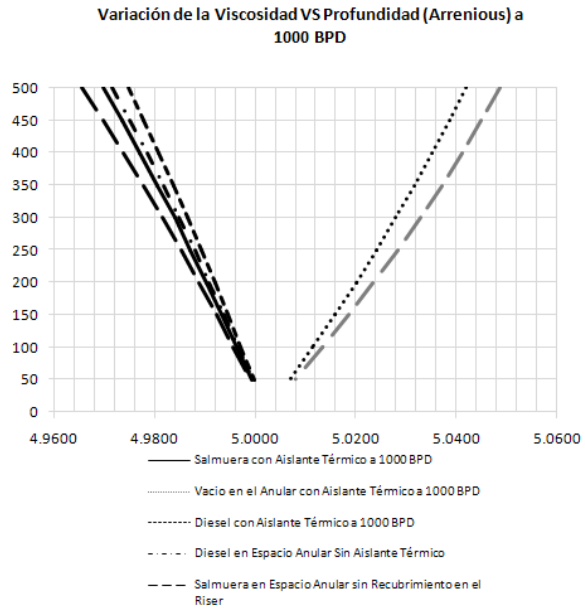

Figure 31 – Behavior of the well producing at 1000 BPD when different packer fluids are in the annular but there is no insulating material around the riser

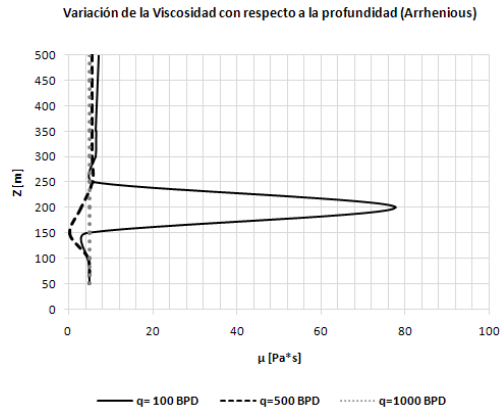

Figure 32 – Behavior of the variation of the viscosity and temperature when there are not fluids in the annular, only exists a presence of air (1)

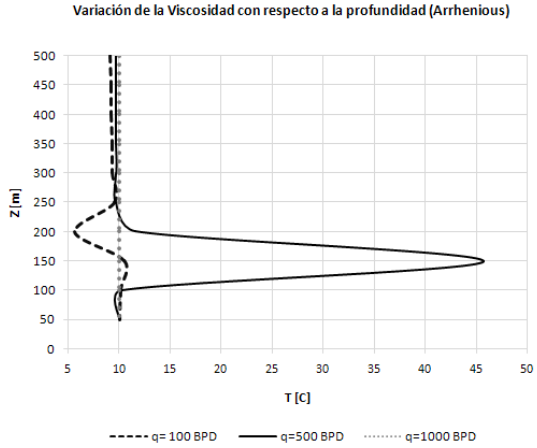

Figure 33 – Behavior of the variation of the viscosity and temperature when there are not fluids in the annular, only exists a presence of air (2)

Association Analysis: Finding Patterns in Email Opt Ins[1]

Halvor Sehested Groenaas, WOTC, Oslo, Norway

Terry Miller, Marketing Communications, Houston-Richmond, US

Introduction

Picture the following everyday scenario. You visit Amazon.com with the intention of buying the latest Harry Potter book. As you enter the Web site, several lists of books pop up that, according to Amazon, should be of interest to you based on your recent viewing history.

As you type in "Harry Potter and the Deathly Hallows", not only do you get hits on the actual book, but also recommendations for other books in the same series, categories (Lord of The Rings, Secret of Narnia, and the like).

How does Amazon do this?

Amazon has developed a system that studies the selections visitors has made in previous visits and use this information to discover patterns, or so-called rules, of customer behavior.

In Schlumberger a similar analysis can be conducted using the email topic opt ins selected by visitors[2].

The concept involves an association analysis that compares the choices visitors make to determine patterns. These patterns help in drawing assumptions about visitor interest and can be used to help create content and/or email campaigns for specific "visitor types" that align with specific patterns. This information can be used to improve Search Engine Optimization and advertising programs and possibly even develop new product/service bundled offerings.

This is achieved through a framework called "Association Rule Analysis." In this paper, we will provide a very basic introduction to Association Rule Analysis, and how it can be applied to mining email topic opt ins for potentially interesting information.

Association Rule Analysis

Association Rule analysis is one of a set of pattern recognition/data mining techniques that automatically look for associations between items that are stored in a "transaction database."

Association rules provide information of this type in the form of "if-then" statements. Unlike the if-then rules of logic, association rules can also attach statistical significance, and other measures of interestingness to the rules.

As an example rule, the output of a "Market basket analysis" of a supermarket database, could yield rules of the form

{Bread, Butter} → { Jam }[3]

This can be read: "**If** a customer buys bread and butter, **then** he/she is also likely to buy jam"

The Association Rule Problem

Let $I=\{i_1, i_2, ..., i_n\}$ be a set a set of binary attributes we call *items*, and let $T=\{t_1, t_2, ..., t_n\}$ be a set of transaction called the *database*. T can be represented as a binary incidence matrix (see Figure 34).

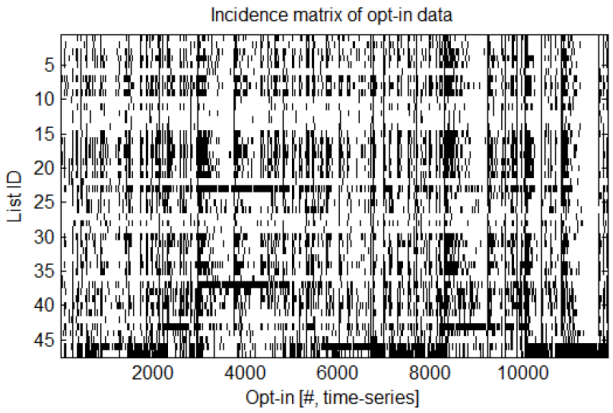

Figure 34 – Incidence matrix of about 10% of the opt-in data set. Black color implies that the registrant opted in for the list. We see that some lists are much less popular than others (white horizontal

[1] **Opt in email** is a term used when someone is given the option to receive "bulk" email, that is, email that is sent to many people at the same time. Typically, this is some sort of mailing list, newsletter, or advertising.

http://en.wikipedia.org/wiki/Opt_in_email

[2] See the list of possible choices at http://www.slb.com/resources/email_subscriptions.aspx

[3] While this example is trivial, other associations might not be so. A famous example of a more surprising association is {Day = Friday, Product = Beer} → { Product = Diapers} !

bands). The white vertical band towards the end of the image is the Christmas/Year-end when there is naturally little activity.

Each transaction contains a subset of items from *I*. An *itemset X* is a set of items from *I*. A transaction, t_i, contains *X* if $X \in t_i$.

The *Support* of an *itemset* is simply the number of times itemset *X* occurs in *T*, divided by the total number of transactions in *T*: $s(X) = \{\#\ incidents\ of\ X\ in\ T\}/\{\#\ transactions\ in\ T\}$. [4]

An *association rule* then is an expression of the form $X \rightarrow Y$, where $X \cap Y = \emptyset$.

The strength of the association rule can be measured in several ways, of which the two most fundamental are the *Support* and the *Confidence*.

The support of a rule, $X \rightarrow Y$, is simply $s(X \cup Y)$. The confidence is given by $s(X \rightarrow Y) = s(X \cup Y)/s(X)$.

Thus the support can be interpreted as the probability, $P(X \cup Y)$, of any given transaction in *T* containing both *X* and *Y*; whereas the confidence is the conditional probability, $P(Y|X)$, that given transaction containing *X*, also will contain *Y*.

Discovering association rules

A given association rule discovery task can thus be defined to "*Find all rules that has a support larger than minsup, and confidence larger than minconf*".

The actual rule discovery typically proceeds in two steps.

1. Find all the *frequent* itemsets satisfying $s(X \rightarrow Y) > minsup$

2. Derive the *strong* rules, $X \rightarrow Y$, satisfying $c(X \rightarrow Y) > minconf$

The first step can be computationally demanding, whereas the second one is typically trivial.

Finding frequent itemsets

For a database containing $|I|$ distinct item types, the possible number of itemsets is $2^{|I|}-1$. Because of this exponential growth, a brute force search is generally not feasible. Amongst others, algorithms for mining frequent itemsets are typically exploiting an important characteristic of the support, $s(\cdot)$, called the *Downward-closure property* (*DCP*). This property guarantees that for a frequent itemset, all its subsets are also frequent and thus for an infrequent itemset, all its supersets must also be infrequent. See Figure 35 for an explanation.

Two canonical algorithms for mining frequent itemsets are the apriori algorithm, and the ECLAT algorithm. Both exploit DCP for efficient searches. The apriori algorithm also derives all the rules as it transverses the data space.

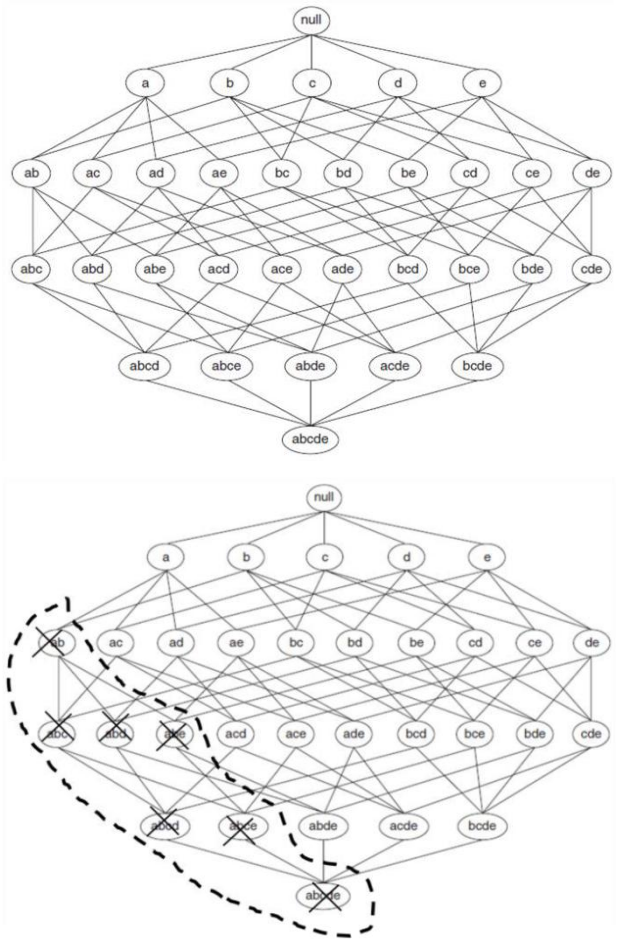

Figure 35 – Incidence Item lattice (up) showing the enumeration of itemsets in a database containing 5 items , {a,b,c,d,e}. Instead of applying the brute-force approach of calculating (counting) the support of every possible itemset in the lattice, we can exploit the downwards-closure property to either prune away supersets of itemsets that we know are below the requested support, or instantly include itemsets that we know will have sufficient support. The example above, we use the knowledge that itemset {ab} has a support less than minsup to remove all super-itemsets of {ab} from the search space at an early stage.

[4] More formally, $Supp(X) = |t_i: X \subseteq t_i, t_i \in T|$

The email optins case revisited

If we go back to the original problem of mining email optins, we have a Webactivity database with 47 different items (newsletter mailing lists), and about 100k transactions (visits). To get an impression of the magnitude of the task of mining this dataset without using a structured approach, the following numbers should help:

At a glance: Combinatorics of the www.slb.com email option data set

- Number of distinct itemsets: ≈ 1.4e14;
- Number of possible rules: ≈ 2.7e22;
- Number of cells in the human body: ≈ 1e14.

By running an R implementation of the ECLAT algorithm on the data, and subsequently forming rules using prespecified minimum support and confidence, we get results similar to those in the table below. These rules can then be used to generate customized Web content, new email campaigns, help in the selection of keywords for Adwords campaigns, and provide data that could indicate a particular Web traffic path that needs to be enriched.

Table 10 – Output from running the ECLAT algorithm on opt in topic data and then forming strong rules

Rules	Support	Confidence
{NT_Schlumberger_Press_Releases} => {NT_Schlumberger_News}	0.162	0.893
{DT_Wireline_Open_Hole} => {DT_Res_Software_Interpretation}	0.149	0.931
{DT_Wellconstruction_Products} => {DT_Intelligent_Completions_Monitoring}	0.122	0.969
{DT_Drill.Bits_Directional_Tools_Services, ,DT_Well_Testing} => {DT_MWD_LWD_MudLogging}		
…	…	…

References

1. • Agrawal, Rakesh; Imielinski, Tomasz; Swami, Arun; Mining Association Rules Between Sets of Items in Large Databases, SIGMOD Conference 1993:207-216.
2. • Piatetsky-Shapiro, Gregory (1991), Discovery, analysis, and presentation of strong rules, in Piatetsky-Shapiro, Gregory; and Frawley, William J.; eds., Knowledge Discovery in Databases, AAAI/MIT Press, Cambridge, MA.
3. • Miller, T. “Using Email Opt-in in Topic Association analysis”. Houston Interactive Marketing Association. 2012.
4. • Tan P-N, Steinbach M, Kumar V. ”Association Analysis: Basic Concepts and Algorithms”. Addison-Wesley, 2006.
5. • Brin, Sergey; Motwani, Rajeev; Ullman, Jeffrey D.; and Tsur, Shalom; Dynamic itemset counting and implication rules for market basket data, in SIGMOD 1997, Proceedings of the ACM SIGMOD International Conference on Management of Data (SIGMOD 1997), Tucson, Arizona, USA, May 1997, pp. 255-264.